Journal of Power Sources 196 (2011) 5918–5921

Contents lists available at ScienceDirect

Journal of Power Sources

journal homepage: www.elsevier.com/locate/jpowsour

Short communication

Effect of gas diffusion layer properties on the time of breakthrough

M. Shahraeeni, M. Hoorfar*

University of British Columbia Okanagan, Kelowna, V1V 1V7, BC, Canada

ARTICLE INFO

Article history:
Received 10 January 2011
Received in revised form 22 February 2011
Accepted 22 February 2011
Available online 6 March 2011

Keywords:
PEM fuel cell
Gas diffusion layer
Fluorescence microscopy
Time of breakthrough
Saturation

ABSTRACT

A visualization technique is employed to measure the time of breakthrough for GDL samples with different characteristics. It is shown that the time of breakthrough is reversely proportional to the hydrophobic content of the GDL sample. The effects of the GDL thickness and injection flow rate on the time of breakthrough are also studied. The results show that the capillary pressure of a thin porous medium is not independent from the time of breakthrough. Thus, it is not legitimate to calculate the saturation of the medium by multiplication of the flow rate and time of breakthrough. These findings help better understanding of flooding phenomena, which may lead to the development of more effective GDLs for PEM fuel cell.

1. Introduction

The agglomeration of liquid water on the interface of the catalyst layer (CL) and the gas diffusion layer (GDL) limits the efficiency of the proton exchange membrane (PEM) fuel cells. Several studies have been conducted to address the flooding phenomenon both numerically and experimentally [1–5]. The experimental studies of flooding have been conducted through in situ and ex situ measurement. In situ measurements mostly consider the effects of GDL characteristics on the total efficiency of the cell [5–7]; while the ex situ visualization techniques examine liquid water motion inside the GDL to understand the details of phenomena underlying flooding [2].

The determination of the capillary pressure and saturation characteristics of the GDL is crucial in evaluating its performance in transferring the liquid water produced on the catalyst layer to the flow channel [8–15]. Benziger et al. [16] measured the breakthrough pressure of different GDL samples using a column of liquid water. They determined the level of saturation by weighting the samples after breakthrough occurred. Loss of water content during disassembling of the GDL sample in each experiment, made the method inaccurate. Büchi et al. [17] employed X-ray tomography to obtain three-dimensional images of liquid water injected into the GDL samples. The size of the samples in X-ray tomography needs to be small; thus, the saturation profiles obtained with this method was unreasonably high. In a series of experiment, Gostick et al. [18] obtained the capillary pressure versus saturation curves for GDL samples with and without microporous layers (MPL). Their results obtained at the point of water breakthrough, which occurs when a sample-spanning cluster of water formed across the GDL, showed that the GDL saturation drastically decreases from 25% to 5% in the presence of MPL [18]. The time Following their previous work, Gostick et al. [19] employed a new approach based on injection of water through GDL using a syringe pump and obtained the variation of water saturation as a function of the capillary pressure at the breakthrough point for treated and untreated GDLs. Assuming that the system has no bubbles and the GDL sample is not flexible, they found the saturation based on the flow rate provided by the syringe pump and the time elapsed from the start of the experiment. Although similar experiments have been conducted by other researchers [2,20,21], none of those cases reports water saturation at breakthrough.

In this paper, we employed the fluorescence microscopy to measure the time required for water to penetrate and travel through the thickness of the GDL. We used Toray carbon papers with different thicknesses (110 μm and 280 μm). For each thickness, GDLs with two types of PTFE loadings (0% and 40 wt.%) were selected. Also, to investigate the effect of the flow rate on the time of breakthrough, the experiments were conducted for three different flow rates: a lower flow rate (5.55×10^{-12} m^3 s^{-1} which is half of the flow rate corresponding to the current density at the flooding condition), the nominal flow rate associated with the flooding (1.11×10^{-11} m^3 s^{-1} for a disk sample with the diameter of 3 mm), and a significantly higher flow rate (i.e., 1.11×10^{-11} m^3 s^{-1}). The results obtained for GDLs with different wettability characteristics show that the capillary pressure of the porous system is not independent from the time of breakthrough. Thus, evaluating the saturation of the sys-

* Corresponding author at: School of Engineering, University of British Columbia Okanagan, Canada. Tel.: +1 250 807 8804; fax: +1 250 807 9850.
E-mail address: mina.hoorfar@ubc.ca (M. Hoorfar).

0378-7753/$ – see front matter © 2011 Elsevier B.V. All rights reserved.
doi:10.1016/j.jpowsour.2011.02.089

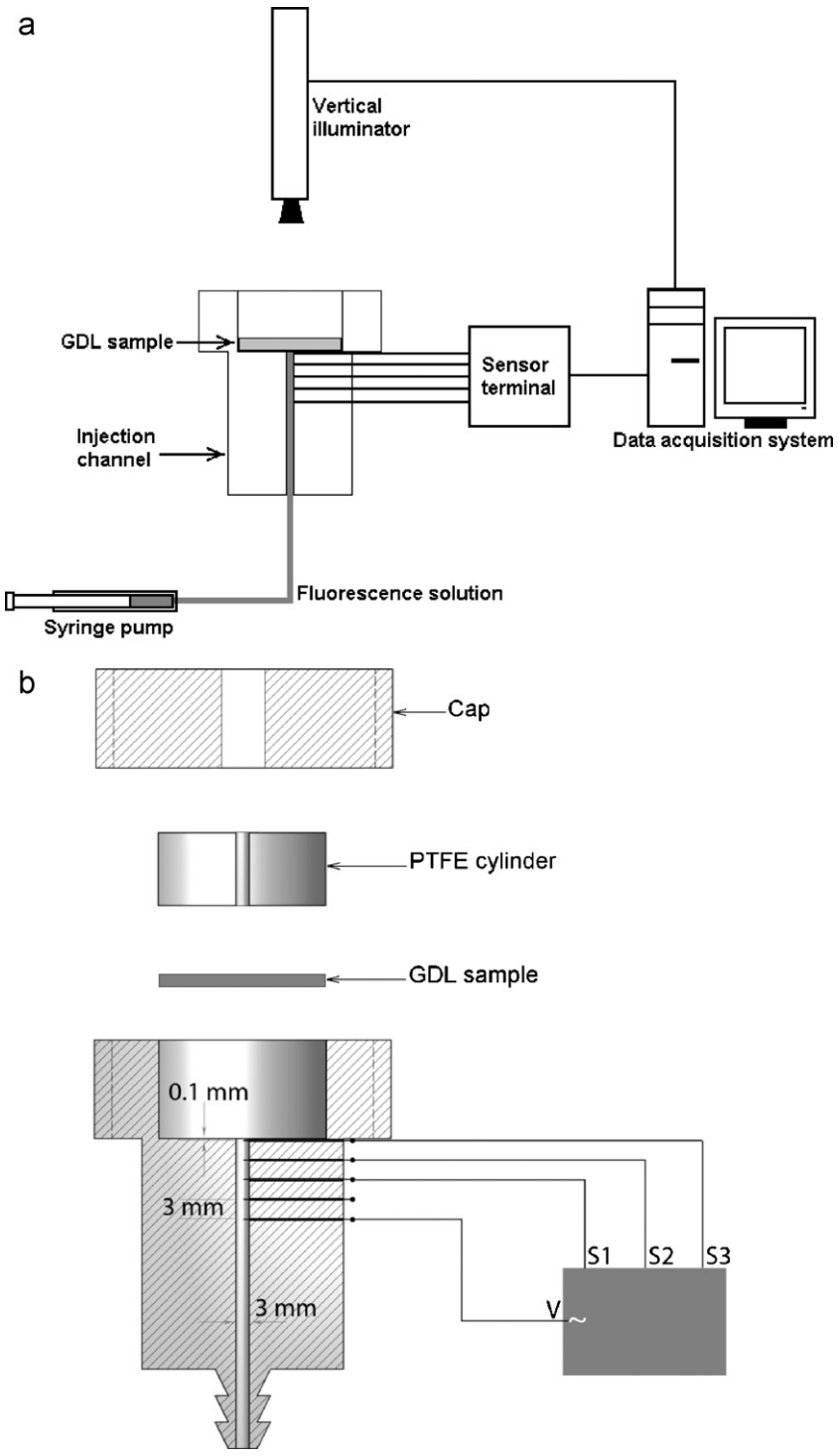

Fig. 1. Schematic of the: (a) experimental setup, (b) injection tube.

tem by multiplication of the flow rate provided by the pump and the time of the breakthrough as proposed by [19] is not accurate.

2. Experimental

In this paper, fluorescence microscopy is employed to visualize water flow inside the GDL and to measure the time of breakthrough. The details of this technique can be found in [2,22]. Fig. 1 illustrates the arrangement of the experimental setup. The fluorescence solution is pumped into the GDL sample via a specially designed device called injection tube made of Teflon. The hydrophobicity of the injection tube prevents any unwanted leakage in the gap between the GDL sample and the surface of the tube. The tube is composed of a 3 mm diameter vertical hole and four horizontal holes with diameter of 300 μm drilled through the tube. Four micro-needles were inserted into the horizontal holes. The arrangement of the needles facilitates the accurate measurement of the flow rate of the solution just before entering the GDL as well as the exact start time of the experiment. In essence, the first needle is to provide voltage to the solution passing through the channel. All three other needles are attached to the voltage sensors. Knowing the distance length between the needles and the time sequence of the signals provided

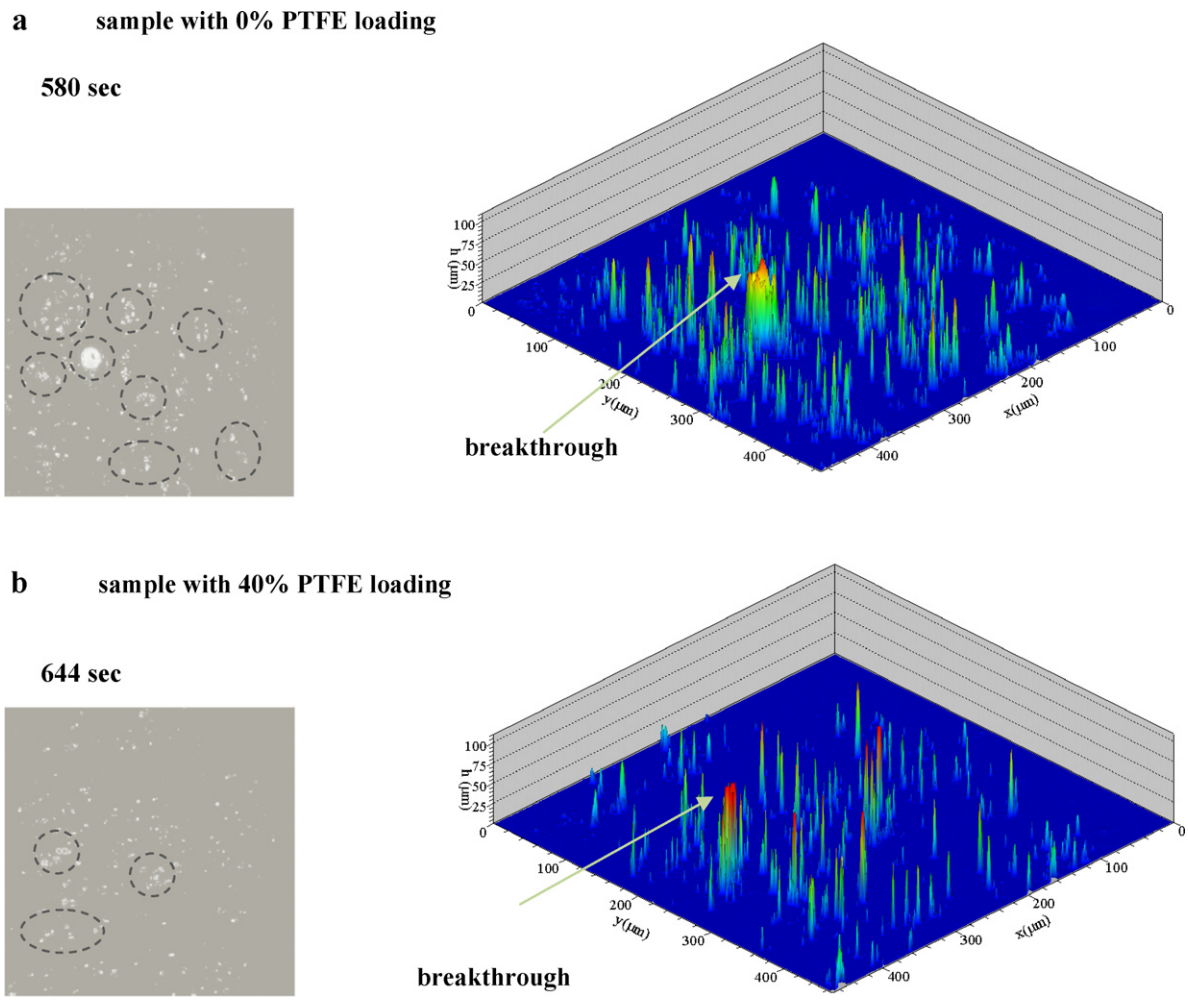

Fig. 2. Breakthrough of water for samples with different PTFE loadings.

by the sensors, the flow rate is estimated. The GDL sample is placed on the top surface of the injection channel and a Teflon cylinder covers the sample. A cap is finally screwed over the cylinder to provide enough pressure on the GDL sample.

3. Results and discussion

Fig. 2(a) and (b) presents the images obtained at the time of breakthrough for two GDL samples with the same thickness (110 μm) but different PTFE loadings (0 wt.% and 40 wt.%). For the sample with no loading, the vast majority of the area is invaded by liquid water (Fig. 2(a)); whereas for the hydrophobic sample, a limited portion of the surface is invaded by water (Fig. 2(b)). Liquid water follows the same pathways after the initial invasion and little new developments occur as time progresses. For the hydrophobic GDL, except for a handful number of pathways, the majority of the GDL is free of water which implies free passages for the reactant gas.

The images obtained from the florescence microscopy were used to obtain a 3D representation of liquid water configuration inside the GDL, especially at the time of breakthrough. The height of the liquid is estimated using the modified correlation proposed by Litster et al. [2]:

$$Z = \frac{110 \times 10^{-6} I}{65535}$$

in which z is the distance from the bottom surface, 110×10^{-6} is the thickness of the sample and I is the intensity of the pixel. The correlation is normalized by the maximum intensity achieved in a 16-bit image data ($2^{16}-1 = 65535$). These 3D representations are used to estimate the water content in each sample by integrating the height of the surface on each pixel. This results presented in Fig. 3 shows that the volume of the liquid in the sample with no PTFE loading is larger than that in the hydrophobic sample as it has been shown before based on the level of saturation [13,15].

The time of breakthrough has also been measured accurately by the signal sent from the needle attached to the lower surface of the GDL. Three replicates of the experiment are carried out for each

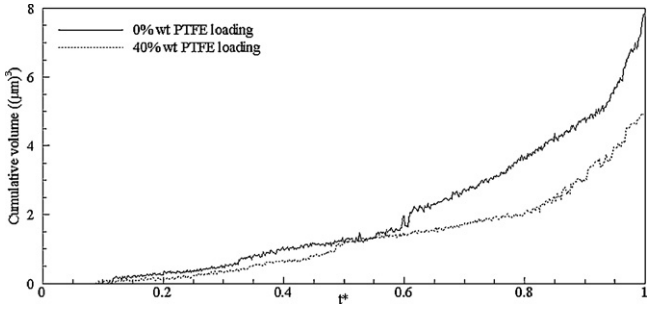

Fig. 3. Cumulative water content versus t^* (i.e., time normalized by the time of breakthrough).

Table 1
Time of breakthrough for the thin sample (TGP-H-30).

Sample type	TGP-H-30 (110 μm)																	
% PTFE	0%									40%								
Flow rate ($m^3\ s^{-1}$)	5.55×10^{-12}			1.11×10^{-11}			1.11×10^{-10}			5.55×10^{-12}			1.11×10^{-11}			1.11×10^{-10}		
Time of BT (s)	1109	1120	996	528	579	584	64	60	53	1049	1164	1187	564	592	655	63	61	57
Average (s)		1075			564			59			1133			604			60	

Table 2
Time of breakthrough for the thick sample (TGP-H-90).

Sample type	TGP-H-90 (280 μm)																	
% PTFE	0%									40%								
Flow rate ($m^3\ s^{-1}$)	5.55×10^{-12}			1.11×10^{-11}			1.11×10^{-10}			5.55×10^{-12}			1.11×10^{-11}			1.11×10^{-10}		
Time of BT (s)	1122	1203	1151	620	601	610	64	68	69	1283	1291	1216	632	701	700	71	67	69
Average (s)		1159			610			67			1263			678			69	

combination of the sample and flow rate. Tables 1 and 2 summarize the time of breakthrough for the combinations. At the lowest and low flow rates (5.55×10^{-12} and $1.11 \times 10^{-11}\ m^3\ s^{-1}$), the effect of thickness is almost the same for both hydrophobic and hydrophilic samples (7.8% and 11.5% for $5.55 \times 10^{-12}\ m^3\ s^{-1}$, and 8.1% and 12.3% for $1.11 \times 10^{-11}\ m^3\ s^{-1}$). As the flow rate is increased by the factor of 10, the time of breakthrough increases for the thick GDL by 13.6% for the hydrophilic and 15% for the hydrophobic samples. This increase is larger than that obtained for the low flow rate cases mentioned above. Thus, it can be concluded that when the flow rate is high, the thickness has a greater effect on the time of breakthrough.

The effect of hydrophobicity on the time of breakthrough is not uniform for different flow rates. For the thin sample, hydrophobicity increases the time of breakthrough by 5.4% at the lowest flow rate. For higher flow rate corresponding to the flooding condition ($1.11 \times 10^{-11}\ m^3\ s^{-1}$), the increase in the time of breakthrough becomes 7.1%. As the flow rate is increased by a factor of 10, the time of breakthrough for the hydrophobic sample is only 1.7% higher than that of hydrophilic sample. The same trend is also observed for the thick sample, i.e., the time of breakthrough is higher for the hydrophobic sample compared to the hydrophilic sample by 8.9%, 11.1% and 2.9% as the flow rate increases. Thus, when the fuel cell is working at the flooding condition, the percentage of PTFE loading has significant effect on conducting liquid water as shown before [9,12,13,15]. The results also show that a simple multiplication of the flow rate by the time of breakthrough as proposed in [19] will give incorrect estimation for saturation as its value for a hydrophobic GDL will be larger than that of a hydrophilic sample.

4. Conclusion

The fluorescence microscopy is employed to investigate the flow of liquid water inside different GDL samples. The effect of PTFE loading studied by analyzing the images captured during the penetration of water inside GDLs with different hydrophobicity and thicknesses. The images show that for the hydrophobic samples, more passages are left free of water and hence available to the reactant gas to reach to the catalyst layer. In addition, the time of breakthrough for different GDL samples were measured and compared. It was shown that the increase in the thickness of the GDL would not necessarily increase the time of the breakthrough proportionally to the thickness. In contrast, treating the GDL with PTFE significantly increases the time of breakthrough. For higher flow rates, the effect of PTFE loading is negligible. It was also shown that the sample with a higher hydrophobic content contains less water than the sample with no loading at the time of breakthrough; while the time of breakthrough for a more hydrophobic sample is larger than that for a sample with no PTFE loading. Therefore, if the relationship proposed in [19] is used to calculate the saturation based on multiplication of the time of breakthrough by the flow rate, the saturation value for the hydrophobic sample will be larger than that of a hydrophilic sample. Thus, it is concluded that the proposed relationship is not valid especially for samples with different wettability characteristics.

References

[1] H. Li, Y. Tang, Z. Wang, Z. Shi, S. Wu, D. Song, J. Zhang, K. Fatih, J. Zhang, H. Wang, J. Power Sources 178 (2008) 103.
[2] S. Litster, D. Sinton, N. Djilali, J. Power Sources 154 (2006) 95.
[3] D. Natarajan, T. Van Nguyen, J. Power Sources 115 (2003) 66.
[4] F.B. Weng, A. Su, C.Y. Hsu, C.Y. Lee, J. Power Sources 157 (2006) 674.
[5] T. Berning, N. Djilali, J. Power Sources 124 (2003) 440.
[6] J. Baschuk, X. Li, J. Power Sources 86 (2000) 181.
[7] F. Barbir, PEM Fuel Cells, 1st ed., Elsevier Academic press, 2006.
[8] O. Chapuis, M. Prat, M. Quintard, E. Chane-Kane, O. Guillot, N. Mayer, J. Power Sources 178 (2008) 258.
[9] J.T. Gostick, M.A. Ioannidis, M.W. Fowler, M.D. Pritzker, J. Power Sources 194 (2009) 433.
[10] J.T. Gostick, M.A. Ioannidis, M.W. Fowler, M.D. Pritzker, J. Power Sources 173 (2007) 277.
[11] J.H. Nam, M. Kaviany, Int. J. Heat Mass Transfer 46 (2003) 4595.
[12] S. Park, J.W. Lee, B.N. Popov, J. Power Sources 177 (2008) 457.
[13] S. Park, B.N. Popov, Electrochim. Acta 54 (2009) 3473.
[14] P.K. Sinha, C.Y. Wang, Electrochim. Acta 52 (2007) 7936.
[15] P.K. Sinha, P.P. Mukherjee, C.Y. Wang, J. Mater. Chem. 17 (2007) 3089.
[16] J. Benziger, J. Nehlsen, D. Blackwell, T. Brennan, J. Itescu, J. Membr. Sci. 261 (2005) 98.
[17] F.N. Büchi, R. Flückiger, D. Tehlar, F. Marone, M. Stampanoni, Proc. 214th ECS Meeting, Honolulu, HI, 12–17 October, 2008.
[18] J.T. Gostick, M.A. Ioannidis, M.W. Fowler, M.D. Pritzker, Electrochem. Commun. 11 (2009) 576.
[19] J.T. Gostick, M.A. Ioannidis, M.D. Pritzker, M.W. Fowler, J. Electrochem. Soc. 157 (2010) 563.
[20] A. Bazylak, D. Sinton, N. Djilali, J. Power Sources 176 (2008) 240.
[21] B. Gao, T.S. Steenhuis, Y. Zevi, J.Y. Parlange, R.N. Carter, T.A. Trabold, J. Power Sources 190 (2009) 493.
[22] J.B. Pawley, B.R. Masters, J. Biomed. Opt. 13 (2008) 29.